Available online at www.sciencedirect.com
SCIENCE DIRECT®
Journal of Theoretical Biology 234 (2005) 341–349
Journal of Theoretical Biology
www.elsevier.com/locate/yjtbi

An individual based model of rippling movement in a myxobacteria population

Alexander R.A. Anderson*, Bakhtier N. Vasiev

Division of Mathematics, University of Dundee, Dundee DD1 4HN, UK

Received 4 November 2004; received in revised form 12 November 2004; accepted 17 November 2004

Abstract

Migrating cells of *Myxococcus xanthus* (MX) in the early stages of starvation-induced development exhibit elaborate patterns of propagating waves. These so-called rippling patterns are formed by two sets of waves travelling in opposite directions. It has been experimentally shown that formation of these waves is mediated by cell–cell contact signalling (C-signalling). Here, we develop an individual-based model to study the formation of rippling patterns in MX populations. Following the work of Igoshin et al. (Proc. Natl. Acad. Sci. 98 (2001) 14913) we consider each moving cell to have an internal clock which controls its turning behaviour and sensitivity to C-signal. Specifically, we examine the effects of changing: C-signal strength, sensitivity/refractoriness, cell density, and noise upon the formation and structure of the rippling patterns. We also consider three modified models that have no explicit refractory period and examine their ability to produce rippling patterns.

Keywords: Myxobacteria; Pattern formation; Cell–cell signalling; Individual-based models

1. Introduction

Myxococcus xanthus (MX) is a Gram-negative rod-shaped bacterium that aggregates to form fruiting bodies when deprived of nutrients. The formation of these multicellular fruiting bodies depends on both temporally and spatially controlled changes in organised cell movements in response to starvation. During the aggregation phase the MX cells pass through a period where the surface is swept by a complex pattern of waves called the ''ripple phase''. This pattern consists of dense ridges of cells moving in opposite directions creating a rippling movement (see Fig. 1). A key question in understanding the ripple pattern concerns the importance of contact-mediated intercellular communication.

MX cells move by gliding, a process whereby bacterial cells move in the direction of their long axes on a solid surface (Henrichsen, 1972). Individual bacteria constantly move and reverse their direction of movement every 5–10 minutes (Jelsbak and Sogaard-Andersen, 1999). The reversal behaviour of MX cells is controlled by cell–cell signalling, specifically MX cells signal via the C-signalling system which operates only when two cells are in end-to-end contact with one another (Kim and Kaiser, 1990; Sager and Kaiser, 1994).

Several models have already been developed to study the formation of the rippling pattern observed in MX bacteria populations (Igoshin et al., 2001; Lutscher and Stevens, 2002; Börner et al., 2002). All of these models assume that C-signalling plays a crucial role in the rippling pattern formation. The models of Igoshin et al. (2001) and Lutscher and Stevens (2002) are continuous partial differential equation models, whilst Börner et al. (2002) deals with a discrete one-dimensional cellular automata model. Both Igoshin et al. (2001) and Börner et al. (2002) assume the existence of a necessary

*Corresponding author. Tel.: +44 1382 344462; fax: +44 1382 345516.
E-mail addresses: anderson@maths.dundee.ac.uk (A.R.A. Anderson), bnvasiev@maths.dundee.ac.uk (B.N. Vasiev).

0022-5193/$ - see front matter © 2005 Elsevier Ltd. All rights reserved.
doi:10.1016/j.jtbi.2004.11.028

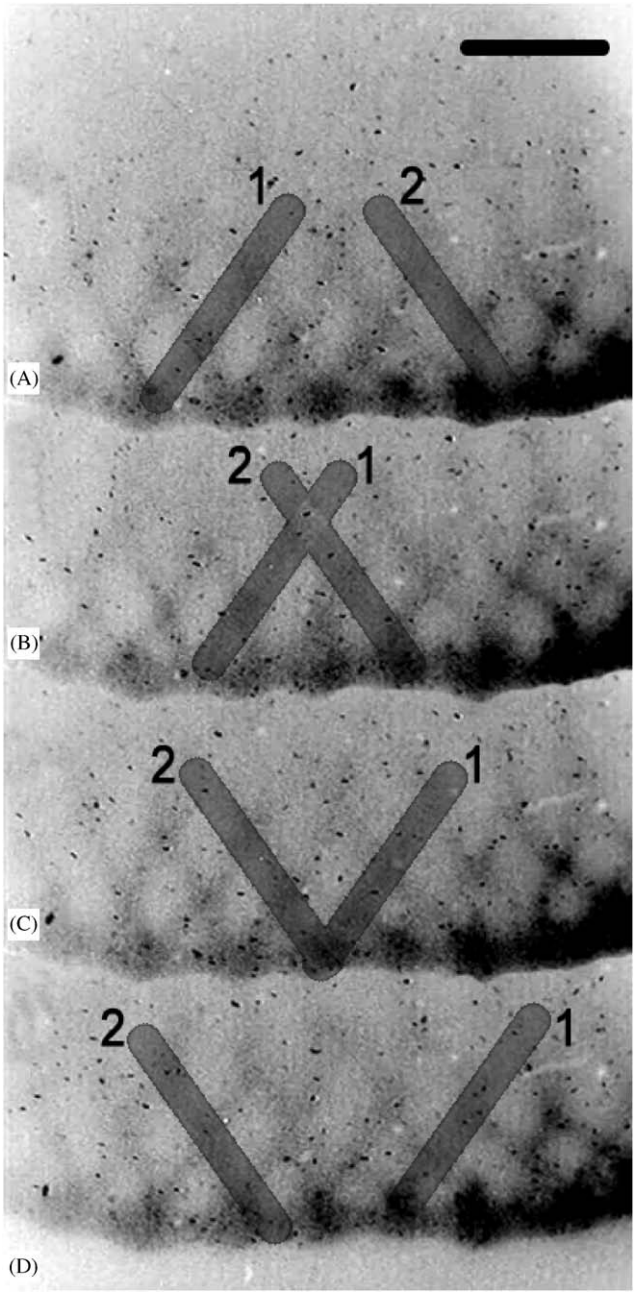

Fig. 1. Dense ridges of cells form during aggregation of MX. These ridges form two sets of travelling waves which appear to move in opposite directions. Four snapshots (A–D) in time of a myxobacteria population during the ripple phase are shown to illustrate this behaviour (ridge 1 moves right and ridge 2 moves left). Figure made from video composite of supplementary movie for Igoshin et al. (2001). Bar on (A) represents 200 μm.

refractory period where, MX bacteria are insensitive to C-signal. With these models if no refractory period exists then no rippling behaviour is observed. The model of Igoshin et al. (2001) also considers the effects of stochasticity on rippling pattern formation and conclude that rippling patterns form only when noise levels are low. Lutscher and Stevens (2002) develop a Goldstein–Kac type model where turning behaviour of cells is described in terms of reaction kinetics. No assumption of a refractory period is required in this model to obtain rippling waves. Another important requirement for formation of rippling patterns pointed out in Igoshin et al. (2001) and Lutscher and Stevens (2002) is a nonlinear dependence of C-signalling on cell density. This was shown by analysis of the model in Lutscher and Stevens (2002) and by numerical study of the model in Igoshin et al. (2001). From these three models we see that the main mechanism generating rippling patterns is an instability caused by nonlinearities in the models (including transition of cells between refractory and sensitive phases).

Whilst the above continuous models were successful in producing rippling patterns and understanding mechanisms of their formation they do not capture the discrete nature of myxobacteria and their interactions. In this sense the model of Börner et al. (2002) is more biologically realistic, however, it over simplifies reversal behaviour of the cells by assuming that a single collision is enough to trigger a reversal.

In this paper we develop a one-dimensional model which combines the advantages of the models of Börner et al. (2002) and Igoshin et al. (2001) in that the cells are considered as individuals and their behaviour is driven by an internal clock. Using this model we examine in detail the conditions under which rippling patterns form and the geometrical properties they exhibit. In particular, we show (i) the existence of standing waves, (ii) there is no necessity for the nonlinear dependence of C-signal on cell density to achieve rippling patterns, (iii) there are irregularities in the rippling patterns and that (iv) these are sensitive to variations in model parameters and noise. Finally, we discuss rippling pattern formation without a refractory period.

2. Model

Our discrete model of rippling pattern formation will consider a number of MX cells distributed in some medium and examine how the distribution of cells varies in time. In addition each cell can have several states which can also change in time. We place the MX cells in continuous space and ignore their size, i.e. we consider each MX cell to be a single point with continuous coordinates. We then apply a few experimentally justified rules for the behaviour of the cells to examine the formation of rippling patterns. We now describe in detail the model assumptions and their justification.

(i) We consider a one-dimensional medium, containing a number of cells. According to experimental observations (Welch and Kaiser, 2001), rippling

waves form in a two-dimensional medium, where the waves are observed as migrating curved ridges of cells. However, it has been shown mathematically (Igoshin et al., 2001; Lutscher and Stevens, 2002; Börner et al., 2002) that the formation of the rippling patterns can be described as a one-dimensional phenomenon.

(ii) Each cell moves either left or right with velocity (v), which is generally constant, this is in agreement with experimental results (Welch and Kaiser, 2001). However, in some of our simulations we will add noise to this constant velocity.

(iii) Each cell is either sensitive or insensitive (refractory) to C-signals from other cells. Whilst there is no direct experimental evidence of a refractory period the work of Sager and Kaiser (1994) hints at its existence, where they showed that high concentrations of isolated C-factor increases the frequency of cell reversals up to some limit (approximately 3 min) which could be the value of refractoriness of the cells. Due to the inconclusive evidence for a refractory period (Igoshin et al., 2001; Börner et al., 2002, Lutscher and Stevens, 2002) we will also consider a modified version of the model that has no explicit refractory period.

(iv) Therefore from (ii), (iii) each cell can be in one of four different states: left or right moving and sensitive or refractory.

(v) Cell state changes periodically (with period $2T$) and is defined by an internal clock (with value ϕ) which increases one unit every time step. The concept of an internal clock was introduced in Igoshin et al. (2001) and is one possible way of modelling the periodic state change behaviour (Fig. 2).

(vi) Cells migrating in opposite directions can come into contact with each other (collide) and exchange C-signal. This assumption is in line with experimental results on contact signalling (Kim and Kaiser, 1990; Sager and Kaiser, 1994).

(vii) Sensitive cells will increase their clock by α units for every collision they receive (α is the C-signal strength). C-signal has been observed to increase reversal frequency of cells (Jelsbak and Sogaard-Andersen, 1999; Welch and Kaiser, 2001; Wenyuan et al., 1996).

Our model is considered as synchronous and therefore all cells are updated at each time step according to the following simulation algorithm:

(i) Each cell relocates, according to the direction and magnitude of its velocity.

(ii) The number of collisions each sensitive cell receives is counted. A collision is defined as when a sensitive cells path crosses the path of any other cell moving in the opposite direction, i.e. for the cells to have crossed paths they must have collided (since our model system is one-dimensional).

(iii) The clock of each cell is increased by one unit. In addition, each collision a sensitive cell receives increases the value of its internal clock by α units.

(iv) Cell state is changed according to its internal clock value (ϕ), i.e. the clock defines whether the cell is left or right moving and sensitive or refractory (see Fig. 2).

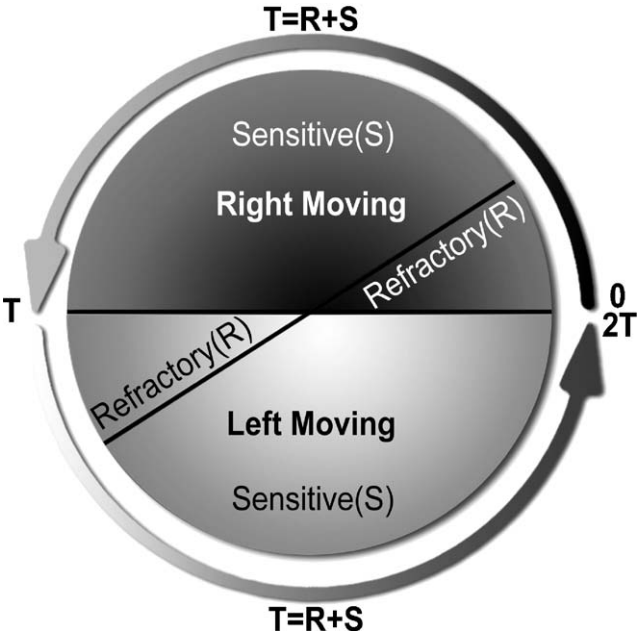

Fig. 2. Schematic diagram of the internal clock that governs cell state and moves anti-clockwise (as signified by the arrows). Cells that have an internal clock value between 0 and $R+S$ (the upper half, darker region) move rightward. While all other cells move leftward (the lower half, lighter region). Cells with internal clock value between 0 and R or between T and $T+R$ are refractory. While cells with internal clock value between R and T or $T+R$ and $2T$ are sensitive. When a cell changes direction its internal clock value is set to 0 (if cell is now left moving) or is set to T (if cell is now right moving).

All simulations start with a number (N) of randomly distributed cells throughout the one-dimensional medium. Initially, each cell has a random value for its internal clock (ϕ) between 0 and $2T$ units, which defines it as either left or right moving and either sensitive or refractory (see Fig. 2). To deal with cells interacting with the boundaries of the medium we impose reflecting boundary conditions, however, we also consider cyclic boundary conditions.

According to experimental observations we shall assume that the cell velocity $v = 10\,\mu\text{m}/\text{min}$, the wavelength of the rippling pattern is 100 μm and the reversal period of cells is approximately 10 min (Welch and Kaiser, 2001). We also know from experimental evidence that the minimum reversal time is 3–4 min

(Sager and Kaiser, 1994), we will assume that this represents the value of the refractory period.

The typical parameter values used in all simulations (unless stated otherwise) were: number of cells $N = 360$, duration of sensitive phase $S = 50$ time units, duration of refractory phase $R = 25$ time units and the strength of C-signal $\alpha = 5.0$. Assuming that 1 time unit = 0.15 min then the refractory period is 3.75 min and a maximum reversal time of 11.25 min.

Since space is considered as continuous then the size of the medium is somewhat arbitrary. However, the size of the medium must be sufficient to contain a few rippling waves. Our typical medium was $L = 800\,\mu m$ which gives a cell density ($\rho = N/L$) of 0.45 cells/μm, although, we examine a range of initial cell densities from 0.01 to 0.5 cells/μm.

3. Results

The main aims of this paper are to examine the parameter space of the model and how properties of observed patterns are affected by changes in these parameters. In the next section we determine the domains where different patterns exist. In Sections 3.2 and 3.3, we study the properties of rippling patterns subject to variation in C-signal strength, cell density and noise. Finally in Section 3.4, we consider three modified models to study the necessity for a refractory period in the formation of rippling patterns.

3.1. Parameter space

In our model we found that three types of patterns can be observed, random waves, standing waves and rippling patterns (see Fig. 3).

Fig. 3A shows the pattern formed by randomly migrating MX cells, this is due to the interactions between the cells not causing synchronisation. From our simulations we observe this pattern when cell density (ρ) or C-signal strength (α) or sensitivity (S) are small (see Fig. 3D). Generally from our results, random waves are observed when $\rho\alpha S < C$, where C is a positive constant of order 1. A decrease in ρ represents a reduction in the number of cells and therefore a reduction in the number of collisions each cell receives every time step. A decrease in α reduces the impact of each collision. A decrease in S reduces the number of time steps available for collisions to occur. Therefore, since only sensitive cells receive C-signal the total impact of collisions on the internal clock value is given by $\rho\alpha S$. Since the internal clock value changes by 1 unit each time step we must have $\rho\alpha S < 1$ for cell–cell interactions to be negligible.

Fig. 3B shows standing waves, when cells form high density stationary clusters. Cells within these clusters continue to move and change direction frequently. The main reason for such rapid changes in direction is due to

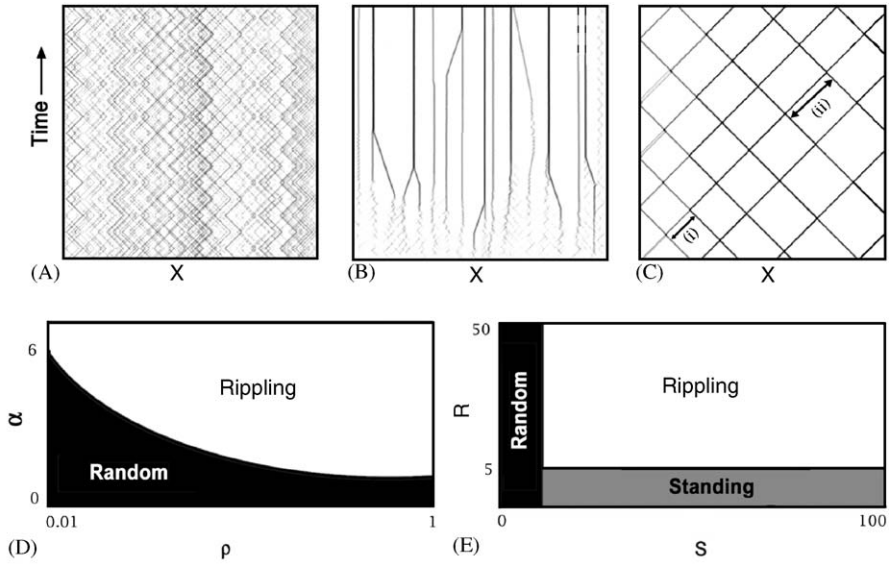

Fig. 3. Space–time plots of the three types of patterns generated by cells in the model. (A) random waves, (B) standing waves and (C) rippling patterns. Dimensions of space–time plots on this and subsequent figures are 800 μm by 60 min. (A) and (B) show first 60 min of simulation and (C) shows stationary pattern of rippling waves after 10 h (4000 time steps). Arrows (i) and (ii) on (C) indicate the wavelength of the rippling pattern in different spatio-temporal locations and show that the wavelength varies over space and time. Grayscale colouring of space–time plots in this (and subsequent figures) represents cell density, i.e. white to black being low to high density. For these (and all subsequent) simulations the parameter values are defined by the typical set of values given in Section 2, unless otherwise stated. $S = 0$ in (A) and $R = 0$ in (B). Parameter space plots of (D) strength of C-signal, α, vs. cell density, ρ, and (E) the duration of refractory period, R, vs. duration of sensitive period, S.

the small refractory period (see Fig. 3E). A characteristic of this pattern is individual clusters of cells that do not interact with one another.

Random waves (Fig. 3A) could be considered as being the resulting pattern from cells that are always insensitive (refractory) and stationary waves (Fig. 3B) could be considered as being the resulting pattern from cells that are always sensitive. These phenomena are at opposite ends of the possible behaviour this model exhibits and somewhere in between we find rippling waves which are the resulting pattern from cells that are neither too sensitive or refractory. Fig. 3C shows the rippling patterns formed by two sets of waves travelling in opposite directions. Therefore the parameter space is divided into three domains, corresponding to random waves, standing waves and rippling patterns (see Fig. 3D and 3E).

3.2. Wavelength distributions

In this paper, we specifically interested in the rippling patterns observed in Fig. 3(C). These patterns form from an initially random distribution of cells which through cell–cell interactions leads to synchronisation of their movements and a clustering of the cells. Cells in each cluster now migrate in synchronisation and produce the characteristic rippling patterns seen in Fig. 3(C).

The periodicity in the rippling patterns can be characterised by wavelength (W). Upon closer inspection we found that there is irregularity in these patterns, i.e. wavelength varies in space and time. As can be seen in Fig. 3(C) we have highlighted two separate regions of the rippling pattern which clearly show different wavelengths. These differences can be described by a distribution of reversal times of all cells. In each cluster cells have approximately the same reversal time, however, cells in different clusters may have different reversal times. Thus each cluster can be characterised by the reversal time of cells forming the cluster and subsequently the wavelength by the moving clusters is given by

$$Wavelength = Cell\ Velocity \times Reversal\ Time,$$

where the velocity (v) is constant. This relationship describes the distance travelled by a single cell for a given reversal time and since all cells in each cluster have the same reversal time it also describes the wavelength of each cluster. Therefore, the distribution of wavelengths for all clusters can be represented by the distribution of reversal times for all clusters. The latter are generated by producing histograms of the time intervals between successive reversals of all cells.

If a cell is refractory it cannot reverse, therefore the minimum period of reversal is bounded by the refractory period (R). On the other hand a cell that receives no collisions will change direction at the end of its sensitive phase, therefore its maximum reversal period will be $R+S$ (see Fig. 2).

Figs. 4 and 5 show different simulations that produced rippling patterns (Figs. 4A–C and 5A–C) correspondingly Figs. 4D–F and 5D–F show the resulting reversal time histograms for each rippling pattern. All histograms confirm our expectation that the wavelength is always in the range: $vR < W < v(S+R)$. However, the actual distribution within this range will be dependent on other model parameters. Note, the above inequality implies that when R is large compared to S the wavelength will grow linearly with R.

The effect of α on the rippling patterns can be seen from Fig. 4. One can see from the space–time plots in Fig. 4A–C that increasing α reduces the wavelength. If α is small the wavelength is close to its maximum value, $R+S$, (Fig. 4D). On the other hand if α is large then the wavelength is close to its minimum value, R, (Fig. 4F). Fig. 4D–F also shows the dispersion in the wavelength distribution for varying α. If α is large (Fig. 4F) or small (Fig. 4D), dispersion is small, however, the dispersion of wavelengths is wider for intermediate values of α (Fig. 4E). Similar results are obtained for varying ρ, i.e. increasing ρ has a similar effect as increasing α. These results imply that the product $\alpha\rho$ will also behave the same way. In reality this product is a measure of the impact of cell–cell interactions. Therefore, these results imply that strong cell interactions results in reversal of cells immediately after the refractory period. Similarly, weak cell interactions results in reversal of cells just before the sensitive phase ends. For intermediate strength cell interactions cells will reverse somewhere between these two extremes and therefore have a wider range of possible reversal times.

3.3. The effects of noise

All biological systems are subject to noise and as such we consider the effects of noise upon the properties of the rippling patterns. In particular, we examine cell velocity noise (with amplitude Z), i.e. only the speed of the cell is effected by noise.

Fig. 5 shows how increasing noise affects the rippling patterns. As noise increases the ridges of cells become more dispersed (Fig. 5A–C) and the rippling pattern becomes more regular (the wavelength becomes more unified over space). The histograms (Fig. 5D–E) also confirm this observation. In addition we can easily see from the histograms that increasing noise increases wavelength.

It seems intuitive that increasing noise in the cell velocity may increase the ridge thickness and decrease dispersion in the wavelength of the resulting rippling patterns. However, the fact that increasing noise further leads to an increase in wavelength might not be so

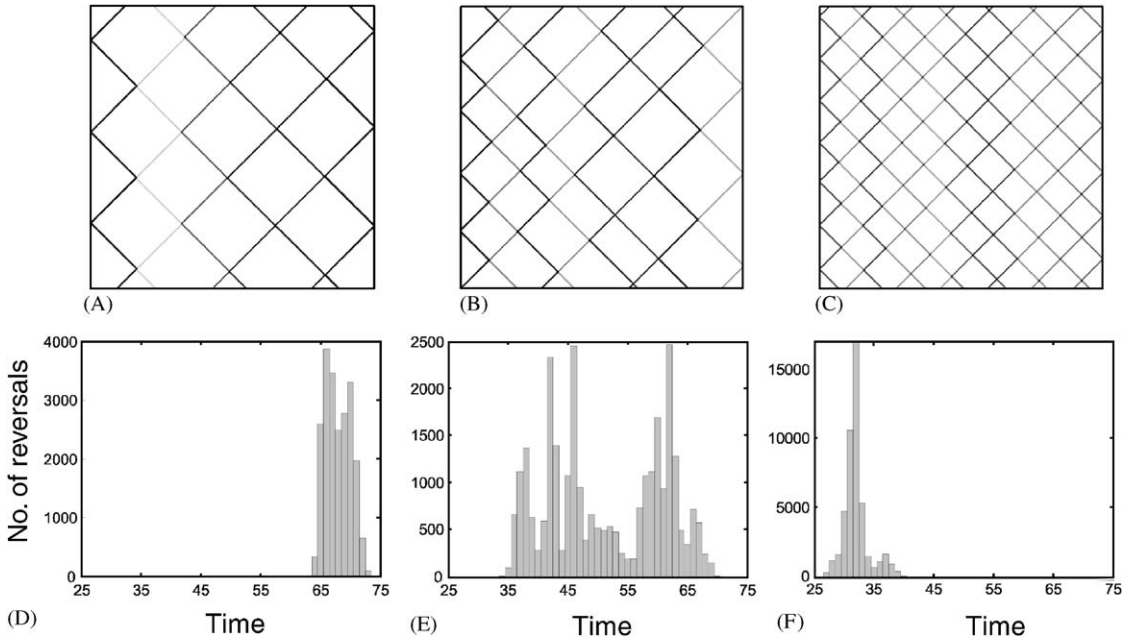

Fig. 4. Space–time plots of the three different rippling patterns generated by cells in the model for increasing values of C-signal strength (α). (A) $\alpha = 1.7$, (B) $\alpha = 5$ and (C) $\alpha = 15$. (D)–(F) are the reversal time histograms corresponding to the rippling patterns in (A)–(C). To produce these (and all subsequent) histograms we waited for 5 h (2000 time steps) for the rippling waves to form and then counted the intervals between cell reversals for all cells for the following 10 h (4000 time steps).

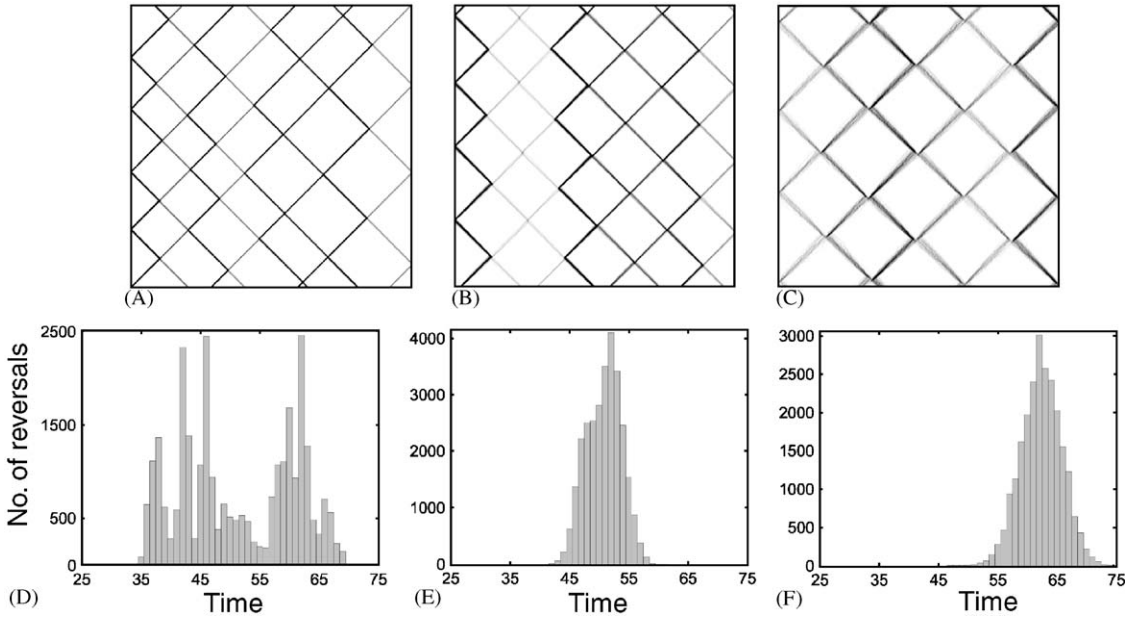

Fig. 5. Space–time plots of the three different rippling patterns generated by cells in the model for increasing values of velocity noise with amplitude Z. (A) $Z = 0.1$, (B) $Z = 0.4$ and (C) $Z = 1.0$. (D)–(F) are the reversal time histograms corresponding to the rippling patterns in (A)–(C).

obvious. This can be explained as follows, an increase in noise will cause some collisions to be missed this will in turn decrease the rate of reversal (i.e. increase the time taken) and therefore increase the wavelength of the rippling patterns.

3.4. Modified model with varying sensitivity

According to our model as well as the models of Igoshin et al. (2001) and Börner et al. (2002) the existence of a refractory state (when cells are insensitive

to C-signals) is an absolute requirement for the formation of rippling patterns. On the other hand the model of Lutscher and Stevens (2002) does not require a refractory period and furthermore there is only indirect experimental evidence for the existence of a refractory cell state (Sager and Kaiser, 1994).

An alternative model to those with a refractory period would possibly consider a modified sensitive period. We have developed a few modifications of the model where sensitivity of cells β is a function of their internal clock value ϕ and examined whether rippling patterns can form in these models. We considered three functions of sensitivity versus internal clock value. In a first modification we used a very steep Hill function with a point of inflection corresponding to the refractory period, $R = 25$, (see Fig. 6). We found that this modification of the model is capable of producing rippling patterns (Fig. 7A). Our original model could be considered as one where the sensitivity of cells to C-signal is changing according to the Heaviside step function (sensitivity versus internal phase): $\beta = 0$ when $\phi < R$ and $\beta = 1$ when $R < \phi < R + S$. The Hill function is very close to this step function and as a result corresponding space–time plots and histograms are very similar (cf. Fig. 4B, E with Fig. 7A, D). Perhaps the most natural way to vary sensitivity is in a linear fashion (Fig. 6). As can be seen from Fig. 7B it also produces rippling patterns with a similar wavelength as before. However, comparing histograms (cf. Fig. 7D and E) we can see a reduced dispersion of the wavelength in the linear case. In the last modification of the model we considered a cubic function of sensitivity versus internal phase. Again this modified model is capable of producing rippling patterns (Fig. 7C, F). From this figure we can see that the wavelength is greatly increased and again the dispersion in wavelength is reduced in comparison with Fig. 7D, E. The plot of the cubic function (Fig. 6) could be considered as corresponding to a model with decreased sensitive and increased

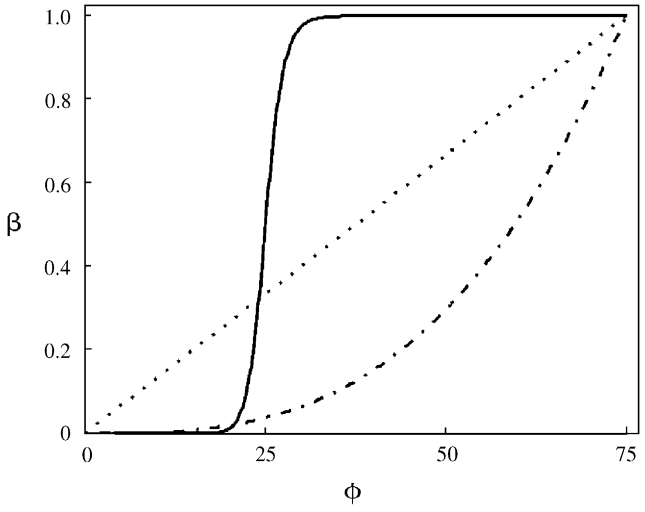

Fig. 6. Plots of the three different functions that are used to vary sensitivity of cells, β, with their internal phase, ϕ, in the non-refractory model (see Fig. 7). The solid line shows a Hill function defined by $\beta_1 = \phi^{20}/((T/3)^{20} + \phi^{20})$, the dotted line is a linear function $\beta_2 = \phi/T$ and dashed–dotted line is a cubic function $\beta_3 = (\phi/T)^3$.

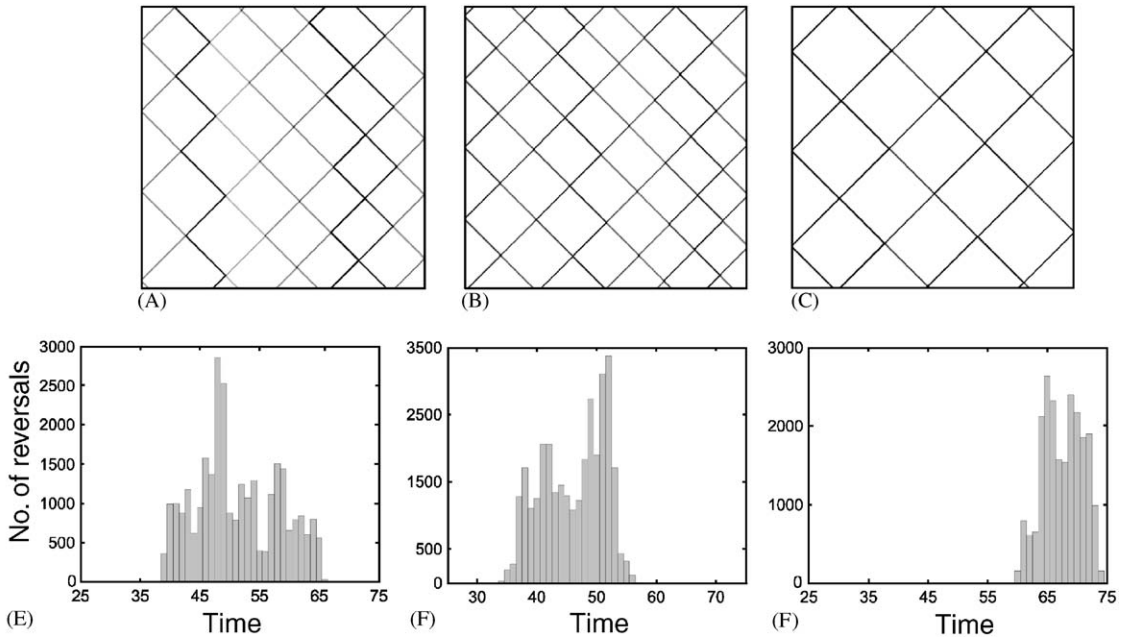

Fig. 7. Space–time plots of the three different rippling patterns generated by cells in three modified models. All of these models have no refractory period and instead have varying sensitivity functions described in Fig. 6. (A) Hill function, (B) linear and (C) cubic. (D)–(F) are the reversal time histograms corresponding to the rippling patterns in (A)–(C).

refractory periods. This explains both the increased wavelength of the rippling pattern and the decreased dispersion observed in Fig. 7C, F.

4. Conclusions and discussion

In this paper we have developed a one-dimensional individual based model of MX bacteria movement and interaction. This model is capable of reproducing the rippling patterns that are observed experimentally in starving populations of MX bacteria (Welch and Kaiser, 2001). We examined in detail the parameter space of this model and found in addition to rippling patterns two other types of waves (Fig. 3). Random waves are observed when cells almost do not interact. Standing waves in contrast are observed when cells are constantly interacting. These two types of wave can be considered as opposite ends of our models behaviour and rippling patterns are somewhere in between.

Rippling waves form regular patterns which can be characterised by their wavelength (see Figs. 4, 5 and 7). This wavelength can vary in both time and space. Rippling wavelength is directly correlated with the reversal frequency of cell movement. Therefore, in order to study the geometry of rippling patterns we produced histograms of the time intervals between successive reversals of all cells. Similar histograms were produced both experimentally and numerically in Igoshin et al. (2001) and Welch and Kaiser (2001). These results showed that histograms from cells producing rippling patterns have a bimodal distribution. This bimodality was explained in terms of the cells location within the wave, where cells are either crest riders or trough travellers. The latter having the longer reversal periods. Comparison of the histograms generated from our model with those of Igoshin et al. (2001) and Welch and Kaiser (2001) shows they are very similar and we often also observe bimodality (Figs. 4, 5 and 7). However, in our model due to its discrete nature there are no trough travellers, as all cells are located on the crests. Therefore our explanation of the observed bimodality must be different. We relate bimodality (or multimodality) to the simple fact that wavelength is not constant over space.

Analysis of the histograms allowed us to examine the effects of varying the model parameters on the rippling patterns. We were then able to show that increasing C-signal strength, α, or increasing density of cells, ρ, decreases the wavelength (Fig. 4) which is in good agreement with experimental observations (Sager and Kaiser, 1994; Welch and Kaiser, 2001; Wenyuan et al., 1996).

In real life the MX population is heterogeneous, i.e. all cells differ slightly in their properties such as speed of migration and C-signal production. To take this into account we introduced noise into our model, specifically we considered velocity noise. Increasing the amplitude of noise, Z, reduced dispersion in wavelength and surprisingly increased wavelength (Fig. 5).

In Igoshin et al. (2001) it was suggested that the formation of rippling patterns is only possible when C-signalling is highly nonlinear, however, we obtain rippling patterns whilst treating C-signalling linearly. Another requirement for the formation of rippling patterns is the existence of a refractory state (Igoshin et al., 2001; Börner et al., 2002). This is also true of our model, since when the refractory period is absent we obtain standing waves (Fig. 3). To analyse this requirement further, we considered three modifications of our model that did not explicitly consider a refractory period but instead considered sensitivity that varied with internal clock value. In all three cases we were able to obtain rippling patterns (Figs. 6 and 7). These results indicate that the need for a refractory period to obtain rippling patterns observed by Igohsin et al. (2001) and Börner et al. (2002) reflects a more general requirement which is a dependence of the sensitivity of cells to C-signal upon internal clock value. Note, the model of Lutscher and Stevens (2002), which has no refractory period, satisfies this requirement. Moreover, in this paper they consider different turning rate functions which are analogous to our phase sensitivity functions (Fig. 6). However, due to the completely different styles of modelling there is no direct way to compare the functions we used to vary sensitivity (Fig. 6) with those of Lutscher and Stevens (2002).

The one-dimensional cellular automata model developed by Börner et al. (2002) could be considered as a limit case of our model where sensitivity, S, tends to infinity and the strength of C-signal, α, is not less than S. In addition our model considers space as continuous while Börner et al. (2002) consider discrete space. Therefore some results we obtained were similar, e.g. for small refractory period we obtain no rippling patterns. However, our model is capable of producing standing waves and we were able to examine the effects of S and α on the properties of the rippling patterns as well as examine the influence of noise.

Following the submission of this manuscript two new publications appeared on modelling pattern formation in myxobacteria populations. In the paper of Alber et al. (2004), a lattice gas cellular automaton was developed which implements cell shape such cells have a biologically realistic dimension, i.e. one cell is made up of several lattice sites in a stick like configuration. The basic assumptions concerning cell behaviour in this model are very similar to ours, except that Alber et al. (2004) take into account a time delay in the cells reversal behaviour. Börner and Bär (2004) developed a continuous reaction–advection model similar to that of Lutscher and Stevens (2002) but with the addition of

time delay which accounts for the refractory period of the myxobacteria. Both of these papers confirm that a refractory period is needed for the formation of rippling patterns.

In laboratory conditions MX populations are essentially two-dimensional where the ridges of the rippling waves are bent at the boundaries. Whilst our one-dimensional model captures much of the observed behaviour in rippling MX populations we would like to develop it further by considering a two-dimensional implementation of our model. Also the life-cycle of MX populations does not stop at rippling waves but progresses to form fruiting bodies. The standing waves, reported in this paper, may be related to the formation of such fruiting bodies. We would therefore like to examine the formation of fruiting bodies in more detail and in particular focus on changes in cell properties between cells forming fruiting bodies and those forming rippling waves.

Acknowledgements

Dr. A.R.A. Anderson was supported by a Personal Research Fellowship from the Royal Society of Edinburgh and an equipment grant from the Royal Society of London. Both authors would like to thank Prof. A. Mogilner for initiating our interest in this field.

References

Alber, S.A., Jiang, Y., Kiskowski, M.A., 2004. Lattice gas cellular automation model for rippling and aggregation in myxobacteria. Physica D. 191, 343–358.

Börner, U., Bär, M., 2004. Pattern formation in a reaction–advection model with delay: a continuum approach to myxobacterial rippling. Ann. Phys. (Leipzig) 13, 432–441.

Börner, U., Deustch, A., Reichenbach, H., Bär, M., 2002. Rippling patterns in aggregates of myxobacteria arise from cell–cell collisions. Phys. Rev. Lett. 89, 078101.

Henrichsen, J., 1972. Bacterial surface translocation: a survey and a classification. Bacteriol. Rev. 36, 478–503.

Igoshin, O.A., Mogilner, A., Welch, R.D., Kaiser, D., Oster G., 2001. Pattern formation and traveling waves in myxobacteria: theory and modeling. Proc. Natl Acad. Sci. 98, 14913–14918.

Jelsbak, L., Sogaard-Andersen, L., 1999. The cell surface-associated intercellular C-signal induces behavioral changes in individual *myxococcus xanthus* cells during fruiting body morphogenesis. Proc. Natl Acad. Sci. 96, 5031–5036.

Kim, S., Kaiser, D., 1990. Cell alignment required in differentiation of *myxococcus xanthus*. Science 249, 2793–2804.

Lutscher, F., Stevens, A., 2002. Emergent patterns in a hyperbolic model for local interacting cell systems. J. Nonlinear Sci. 12, 619–640.

Sager, B., Kaiser, D., 1994. Intercellular C-signaling and the traveling waves of *myxococcus*. Genes Dev. 8, 2793–2804.

Welch, R., Kaiser, D., 2001. Cell behavior in traveling wave patterns of myxobacteria. Proc. Natl Acad. Sci. 98, 14907–14912.

Wenyuan, S., Ngok, F., Zusman, D., 1996. Cell density regulates cellular reversal frequency in *myxococcus xanthus*. Proc. Natl Acad. Sci. 93, 4142–4146.